Paper

Robust LFC in a Deregulated Environment : Multi-objective Control Approach

Hassan Bevrani* Student Member
Yasunori Mitani** Member
Kiichiro Tsuji* Member

This paper addresses a new decentralized robust load-frequency control (LFC) design in a multi-area power system under deregulation based on bilateral policy scheme. In each control area, the effect of bilateral contracts is taken into account as a set of new input signals to modify the traditional LFC structure. The LFC problem is considered as a multi-objective control problem and formulated via a mixed H_2/H_∞ control technique, then it is easily carried out to synthesis the desired low-order robust controllers by solving standard linear matrix inequalities (LMI). A three-area power system example with possible contract scenarios and a wide range of load changes is given to illustrate the developed approach. The results of the proposed multi-objective control strategy are compared with pure H_∞ design. The resulting controllers are shown to maintain the robust performance and minimize the effect of disturbances and specified uncertainties.

Keywords: Load frequency control, mixed H_2/H_∞ control, restructured power system, robust performance

1. Introduction

In a deregulated environment, load-frequency control (LFC) as an ancillary service acquires a fundamental role for maintaining the electrical system reliability at an adequate level. That is why there has been increasing interest for designing load frequency controllers with better performance according to changing environment of power system operation under deregulation. Recently, several reported strategies attempted to adapt well tested classical LFC schemes for restructured power system [(1)~(6)]. The main advantage of these strategies is in using the basic concepts of traditional framework and avoiding from apply the impractical or untested LFC models. Following mentioned attempts, this paper addresses a novel control strategy for the generalized LFC structure which is presented in Ref. (5) (6). The introduced generalized LFC model shows how the bilateral contracts are incorporated in the traditional LFC system leading to a new model.

Naturally, LFC is a multi-objective control problem. LFC goals i.e. frequency regulation and tracking the load changes, maintaining the tie-line power interchanges to specified values in presence of generation constraints and dynamical model uncertainties, determines the LFC synthesis as a multi-objective control problem. Therefore, it is expected that an appropriate multi-objective control strategy could be able to give a better solution for this problem. However, in the reported robust LFC approaches, for example Ref. (7)∼(9), only one single norm is used to capture design specifications. It is clear that meeting all the LFC design objectives by a single norm-based control approach with regard to increasing the complexity and changing of power system structure is difficult. Furthermore each robust method is mainly useful to capture a set of special specifications. For instance, the regulation against random disturbances more naturally can be addressed by LQG or H_2 synthesis. The H_2 tracking design is more adapted to deal with transient performance by minimizing the linear quadratic cost of tracking error and control input, but H_∞ approach (and μ as a generalized H_∞ approach) is more useful to holding closed-loop stability in presence of control constraints and uncertainties.

While the H_∞ norm is natural for norm-bounded perturbations, in many applications the natural norm for the input-output performance is the H_2 norm. It is shown that using the combination of H_2 and H_∞ (mixed H_2/H_∞) allows a better performance for a control design problem including both set of above objectives [(10)].

In this paper, first the LFC problem is formulated as a multi-objective control problem for a given generalized control area with several generation units in a deregulated environment and then it is solved by a mixed H_2/H_∞ control approach to obtain the desired robust decentralized controller. The model uncertainty in each control area is covered by an unstructured multiplicative uncertainty block. The proposed strategy is applied to a three-control area example to design a set of robust low-order controllers. The results of the proposed multi-objective approach are compared with the proposed dynamic pure H_∞ controllers, which show the effectiveness of this methodology. The preliminary steps of this work are presented in Ref. (5) (6).

2. Bilateral-based LFC Scheme [(5)]

In a deregulated environment, vertically integrated utilities

* Department of Electrical Eng., Graduate School of Eng., Osaka University
2-1, Yamada-Oka, Suita 565-0871
** Department of Electrical Eng., Kyushu Institute of Technology
1-1, Sensuicho, Tobata-ku, Kitakyushu 804-8550

no longer exist, however the common objectives, i.e. restoring the frequency and the net interchanges to their desired values for each control area are remained. In Ref. (5), a traditional-based dynamical model is generalized for a given control area in deregulated environment under bilateral LFC scheme, following the idea presented in Ref. (3). This section gives a brief overview of generalized LFC model which uses all the information required in a vertically operated utility industry plus the contract data information.

Based on the mentioned model, overall power system structure can be considered as a collection of distribution companies (Discos) or control areas interconnected through high voltage transmission lines or tie-lines. Each control area has its own LFC and is responsible for tracking its own load and honoring tie-line power exchange contracts with its neighbors. There can be various combinations of contracts between each Disco and available generation companies (Gencos). On the other hand each Genco can contract with various Discos. The "generation participation matrix (*GPM*)" concept is defined to express these bilateral contracts in the generalized model. *GPM* shows the participation factor of each Genco in the considered control areas and each control area is determined by a Disco. The rows of a *GPM* correspond to Gencos and columns to control areas which contract power. For example, for a large scale power system with m control area (Discos) and n Gencos, the GPM will have the following structure. Where gpf_{ij} refers to "generation participation factor" and shows the participation factor of Genco i in the load following of area j (based on a specified bilateral contract).

$$GPM = \begin{bmatrix} gpf_{11} & gpf_{12} & \cdots & gpf_{1(m-1)} & gpf_{1m} \\ gpf_{21} & gpf_{22} & \cdots & gpf_{2(m-1)} & gpf_{2m} \\ \vdots & \vdots & \vdots & \vdots & \vdots \\ gpf_{(n-1)1} & gpf_{(n-1)2} & \cdots & gpf_{(n-1)(m-1)} & gpf_{(n-1)m} \\ gpf_{n1} & gpf_{n2} & \cdots & gpf_{n(m-1)} & gpf_{nm} \end{bmatrix} \quad \cdots\cdots (1)$$

A generalized LFC block diagram for control area i can be obtained in a deregulated environment as shown in Fig. 1. New information signals due to possible various contracts between Disco i and other Discos and Gencos are shown as dashed-line inputs, and, we can write [5]:

$$v_{1i} = \Delta P_{Loc-i} + \Delta P_{di} \quad \cdots\cdots (2)$$

$$v_{2i} = \sum_{\substack{j=1 \\ j\neq i}}^{N} T_{ij}\Delta f_j \quad \cdots\cdots (3)$$

$$v_{3i} = \sum (Total\ export\ power - Total\ import\ power)$$
$$= \sum_{\substack{j=1 \\ j\neq i}}^{N} \left(\sum_{k=1}^{n} gpf_{kj}\right)\Delta P_{Lj} - \sum_{k=1}^{n}\left(\sum_{\substack{j=1 \\ j\neq i}}^{N} gpf_{jk}\right)\Delta P_{Li} \quad \cdots\cdots (4)$$

$$v_{4i} = \begin{bmatrix} v_{4i-1} & v_{4i-2} & \cdots & v_{4i-n} \end{bmatrix} \quad \cdots\cdots (5)$$

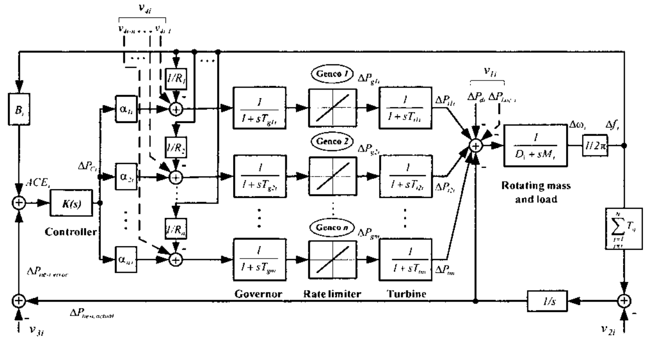

Fig. 1. Generalized LFC model in a deregulated environment

$$v_{4i-1} = \sum_{j=1}^{N} gpf_{1j}\Delta P_{Lj}$$
$$\vdots \quad \cdots\cdots (6)$$
$$v_{4i-n} = \sum_{j=1}^{N} gpf_{nj}\Delta P_{Lj}$$

$$\Delta P_{tie-i,error} = \Delta P_{tie-i,actual} - v_{3i} \quad \cdots\cdots (7)$$

$$\sum_{i=1}^{n} gpf_{ij} = 1 \quad \cdots\cdots (8)$$

$$\sum_{k=1}^{n} \alpha_{ki} = 1; \quad 0 \leq \alpha_{ki} \leq 1 \quad \cdots\cdots (9)$$

$$\Delta P_{mi} = \sum_{j=1}^{N} gpf_{ij}\Delta P_{Lj} \quad \cdots\cdots (10)$$

Where, Δf_i: frequency deviation, ΔP_{gi}: governor valve position, ΔP_{ci}: governor load setpoint, ΔP_{ti}: turbine power, ΔP_{tie-i}: net tie-line power flow, ΔP_{di}: area load disturbance, M_i: equivalent inertia constant, D_i: equivalent damping coefficient, T_{gi}: governor time constant, T_{ti}: turbine time constant, T_{ij}: tie-line synchronizing coefficient between area i & j, B_i: frequency bias, R_i: drooping characteristic, α: ACE participation factor, N: number of control areas, ΔP_{Li}: contracted demand of area i, ΔP_{mi}: power generation of a Genco i, ΔP_{Loc-i}: total local demand (contracted and uncontracted) in area i, v_{3i}: scheduled $\Delta P_{tie-i}(\Delta P_{tie-i,scheduled})$ and $\Delta P_{tie-i,actual}$: actual ΔP_{tie-i}.

Interested readers can find more details on above LFC modeling and simulation for a given restructured power system in Ref. (3) (5).

3. Problem Formulation and Control Strategy

The main control framework in order to formulate the LFC problem via a mixed H_2/H_∞ control design for a given control area (Fig. 1) is shown in Fig. 2. The removed part of block diagram (right hand) is the same as in Fig. 1. In Fig. 2, Δ_i models the structured uncertainty set in the form of multiplicative type and W_i includes the associated weighting function. The output channel $z_{\infty i}$ is associated with the H_∞ performance while the fictitious output z_{2i} contains $z_{2i}(1)$, $z_{2i}(2)$ and $z_{2i}(3)$ is associated with LQG aspects or H_2 performance.

The η_{1i}, η_{2i} and η_{3i} in Fig. 2 are constant performance weighting coefficients. Experience suggests that one can

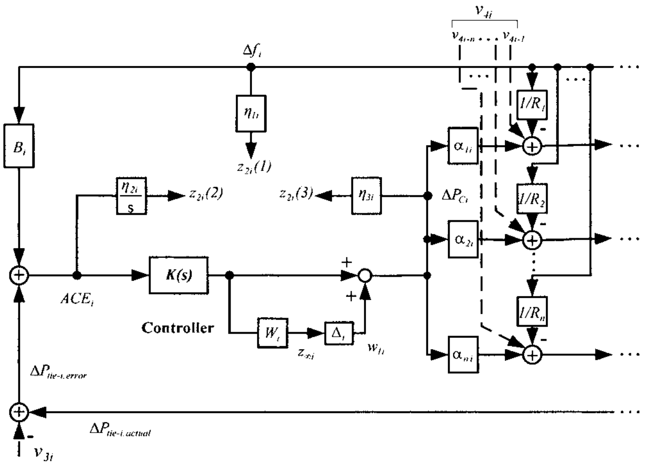

Fig. 2. Proposed control strategy

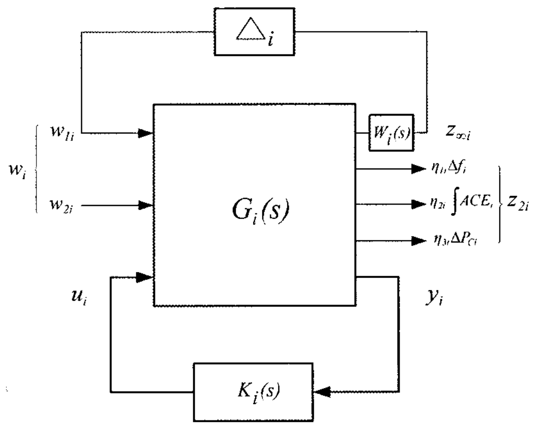

Fig. 3. Mixed H_2/H_∞-based control framework

fix the weights η_{1i}, η_{2i} and η_{3i} to unity and use the method with regional pole placement technique for performance tuning[11]. We can redraw Fig. 2 as shown in Fig. 3, where $G_i(s)$ and $K_i(s)$ correspond to the nominal dynamical model of the given control area and controller, respectively. Also y_i is the measured output, u_i is the control input and w_i includes the perturbed and disturbance signals in the control area.

The LFC problem as a multi-objective control problem can be expressed by the following optimization problem: design a controller that minimizes the 2-norm of the fictitious output signal z_{2i} under the constraints that the ∞-norm of the transfer function from w_{1i} to $z_{\infty i}$ is less than one. On the other hand, the LFC design is reduced to find an internally stabilizing controller K_i which minimizes

$\left\|T_{z_{2i}w_{2i}}\right\|_2$ while maintaining $\left\|T_{z_{\infty i}w_{1i}}\right\|_\infty < 1$.

This problem can be solved by convex optimization using linear matrix inequalities. Interested readers can find enough details on the related technical background in Ref. (12) (13). According to Fig. 1 and the proposed control framework (Fig. 3), the state space model for control area i, $G_i(s)$, can be obtained as

$$\left.\begin{aligned} \dot{x}_i &= A_i x_i + B_{1_i} w_i + B_{2_i} u_i \\ z_{\infty i} &= C_{\infty i} x_i + D_{\infty 1_i} w_i + D_{\infty 2_i} u_i \\ z_{2i} &= C_{2i} x_i + D_{21_i} w_i + D_{22_i} u_i \\ y_i &= C_{yi} x_i + D_{y1_i} w_i \end{aligned}\right\} \cdots\cdots\cdots\cdots\cdots (11)$$

where

$$x_i^T = \left[\Delta f_i \quad \Delta P_{tie-i} \quad \int ACE_i \quad x_{ti} \quad x_{gi}\right] \cdots\cdots\cdots (12)$$

$$x_{ti} = \left[\Delta P_{t1i} \quad \Delta P_{t2i} \quad \cdots \quad \Delta P_{tni}\right] \cdots\cdots\cdots\cdots (13)$$

$$x_{gi} = \left[\Delta P_{g1i} \quad \Delta P_{g2i} \quad \cdots \quad \Delta P_{gni}\right] \cdots\cdots\cdots\cdots (14)$$

$$w_i^T = \left[w_{1i} \quad w_{2i}\right], \quad w_{2i}^T = \left[v_{1i} \quad v_{2i} \quad v_{3i} \quad v_{4i}\right] \cdots\cdots\cdots\cdots\cdots (15)$$

$$v_{4i}^T = \left[v_{4i-1} \quad v_{4i-2} \quad \cdots \quad v_{4i-n}\right]$$

$$u_i = \Delta P_{Ci}, \quad y_i^T = \left[ACE_i \quad \int ACE_i\right] \cdots\cdots\cdots (16)$$

$$z_{2i}^T = \left[\eta_{1i}\Delta f_i \quad \eta_{2i}\int ACE_i \quad \eta_{3i}\Delta P_{Ci}\right] \cdots\cdots\cdots (17)$$

and,

$$A_i = \begin{bmatrix} A_{i11} & A_{i12} & A_{i13} \\ A_{i21} & A_{i22} & A_{i23} \\ A_{i31} & A_{i32} & A_{i33} \end{bmatrix}, \quad B_{1i} = \begin{bmatrix} B_{1i11} & B_{1i12} \\ B_{1i21} & B_{1i22} \\ B_{1i31} & B_{1i32} \end{bmatrix},$$

$$B_{2i} = \begin{bmatrix} B_{2i1} \\ B_{2i2} \\ B_{2i3} \end{bmatrix} \quad A_{i11} = \begin{bmatrix} -D_i/2\pi M_i & -1/2\pi M_i & 0 \\ \sum_{\substack{j=1 \\ j\neq i}}^{N} T_{ij} & 0 & 0 \\ B_i & 1 & 0 \end{bmatrix},$$

$$A_{i12} = \begin{bmatrix} 1/2\pi M_i & \cdots & 1/2\pi M_i \\ 0 & \cdots & 0 \\ 0 & \cdots & 0 \end{bmatrix}_{3\times n}$$

$$A_{i22} = -A_{i23} = diag\left[-1/T_{t1i} \; -1/T_{t2i} \cdots -1/T_{tni}\right]$$

$$A_{i33} = diag\left[-1/T_{g1i} \quad -1/T_{g2i} \quad \cdots \quad -1/T_{gni}\right]$$

$$A_{i31} = \begin{bmatrix} -1/(T_{g1i}R_{1i}) & 0 & 0 \\ \vdots & \vdots & \vdots \\ -1/(T_{gni}R_{ni}) & 0 & 0 \end{bmatrix},$$

$$A_{i13} = {A_{i21}}^T = 0_{3\times n}, \quad A_{i32} = 0_{n\times n}$$

$$B_{1i12} = \begin{bmatrix} -1/2\pi M & 0 & 0 & 0 & \cdots & 0 \\ 0 & -1 & 0 & 0 & \cdots & 0 \\ 0 & 0 & -1 & 0 & \cdots & 0 \end{bmatrix}_{3\times(3+n)},$$

$$B_{1i32} = \left[0_{n\times 3} \; b\right] \quad b = diag\left[1/T_{g1i} \; 1/T_{g2i} \cdots 1/T_{gni}\right],$$

$$B_{1i11} = 0_{3\times 1}, \quad B_{1i21} = 0_{n\times 1}$$

$$B_{1i22} = 0_{n\times(3+n)}, \quad B_{2i1} = 0_{3\times 1}, \quad B_{2i2} = 0_{n\times 1}$$

$${B_{2i3}}^T = \left[\alpha_{1i}/T_{g1i} \quad \alpha_{2i}/T_{g2i} \quad \cdots \quad \alpha_{ni}/T_{gni}\right]$$

$${B_{1i31}}^T = \left[\alpha_{1i}/T_{g1i} \quad \alpha_{2i}/T_{g2i} \quad \cdots \quad \alpha_{ni}/T_{gni}\right]$$

$$C_{\infty i} = 0_{1\times(2n+3)}, \quad D_{\infty 1i} = \left[-1 \quad 0_{1\times(3+n)}\right], \quad D_{\infty 2i} = 1$$

$$C_{2i} = \left[c_{2i1} \; c_{2i2}\right], \; c_{2i1} = \begin{bmatrix} \eta_{1i} & 0 & 0 \\ 0 & 0 & \eta_{2i} \\ 0 & 0 & 0 \end{bmatrix}, \; c_{2i2} = 0_{3\times 2n}$$

$$D_{21i} = 0_{3\times(4+n)}, \quad D_{22i} = \begin{bmatrix} 0 \\ 0 \\ \eta_{3i} \end{bmatrix}$$

$$C_{yi} = \left[c_{yi} \; 0_{2\times 2n}\right], \; c_{yi} = \begin{bmatrix} \beta_i & 1 & 0 \\ 0 & 0 & 1 \end{bmatrix}, \; D_{y1i} = 0_{2\times(4+n)}.$$

The proposed control framework covers all mentioned LFC objectives. The H_2 performance is used to minimize the effects of disturbances on area frequency and area control error (ACE) by introducing fictitious controlled outputs

$z_{2i}(1)$ and $z_{2i}(2)$. In result, the tie-line power flow (which can be described as a linear combination of frequency deviation and ACE signals) is controlled. Furthermore, fictitious output $\eta_{3i}\Delta P_{Ci}$ sets a limit on the allowed control signal to penalize fast changes and large overshoot in the governor load set-point with regards to corresponded practical constraint on power generation by generator units. Also in LFC, it is important to keep up the frequency regulation and desired performance in the face of uncertainties affecting the control area [14]. The H_∞ performance is used to meat the robustness against specified uncertainties and reduction of its impact on closed-loop system performance. Therefore, it is expected that the proposed strategy satisfy the main objectives of LFC system under load disturbance and model uncertainties.

Following a load disturbance within a control area, the frequency of that area experiences a transient change, the feedback mechanism comes into play and generates appropriate rise/lower signal to the participated Gencos according to their participation factors (α_{ji}) and contract information (GPM) to make generation follow the load. In the steady state, the generation is matched with the load, driving the tie-line power and frequency deviations to zero.

The balance between connected control areas is achieved by detecting the frequency and tie line power deviations to generate the area control error (ACE) signal which is turn utilized in the proposed control strategy as shown in Fig. 1. The ACE for each control area can be expressed as a linear combination of tie-line power change and frequency deviation.

$$ACE_i = B_i \Delta f_i + \Delta P_{tie-i} \quad \cdots\cdots (18)$$

Where, B_i is frequency bias coefficient. Although in the LFC literature, B_i is considered as a fixed value, however currently estimating of its value on a real-time basis is an open research area. In any case, with fixed bias coefficient, the impact on ACE from external disturbances should not be ignored [15].

In the next section, two sets of robust controllers are developed for a power system example including three control areas. The first one includes designed reduced-order controllers based on the proposed mixed H_2/H_∞ approach and the second one contains pure H_∞ controllers based on general LMI technique with the assumed same objectives and initializations to achieve desired robust performance.

4. A 3-Control Area Example

To illustrate the effectiveness of proposed control strategy, a three control area power system, shown in Fig. 4, is considered as a test system. It is assumed that $\alpha_{ji} = 0.333$ and [D_i (pu/Hz), M_i (pu.sec)] for areas 1 to 3 are [0.044, 0.4867], [0.044, 0.5477] and [0.046, 0.4784] respectively. The rate limit value for each Genco is assumed 0.1. The other power system parameters are considered to be the same as in Ref. (9).

4.1 Weights Selection In this example with regards to uncertainty, it is assumed that the parameters of rotating mass and load pattern in each control area have uncertain values. The variation range for D_i and M_i parameters is assumed ±20%. Considering the more complete model by including additional uncertainties is possible and causes less

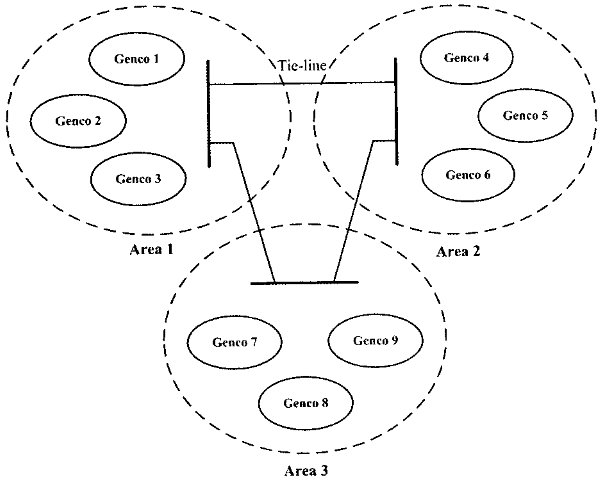

Fig. 4. 3-Control area power system

conservative in synthesis. However, the complexity of computations and the order of resulted controller will increase. These uncertainties are modeled as an unstructured multiplicative uncertainty block that contains all the information available about D_i and M_i variations. Corresponding to an uncertain parameter, let $\hat{G}_i(s)$ denotes the transfer function from the control input u_i to control output y_i at operating points other than nominal point. Then the multiplicative uncertainty block can be expressed as

$$|\Delta_i(s)W_i(s)| = \left|[\hat{G}_i(s) - G_{0i}(s)]G_{0i}(s)^{-1}\right|; G_{0i}(s) \neq 0 \quad \cdots\cdots (19)$$

where, $\|\Delta_i(s)\|_\infty = sup_\omega |\Delta_i(s)| \leq 1$.
$\Delta_i(s)$ shows the uncertainty block corresponding to uncertain parameter and $G_{0i}(s)$ is the nominal transfer function model.

Thus, $W_i(s)$ is such that its respective magnitude bode plot covers the bode plots of all possible plants. For example, using Eq. (19), some sample uncertainties corresponding to different values of D_i and M_i for area 1 are shown in Fig. 5. It can be seen the frequency responses of both set of parametric uncertainties are close to each other, and, hence to keep the complexity of obtained controller low, we can model uncertainties due to both set of parameters variation by using a norm bonded multiplicative uncertainty to cover all possible plants as follows

$$W_1(s) = \frac{0.3063s + 0.053}{s + 0.5338} \quad \cdots\cdots (20)$$

Fig. 5 clearly shows that attempting to cover the uncertainties at all frequencies and finding a tighter fit (in low frequencies) using higher order transfer function will result in high-order controller. This weight (Eq. (20)) gives a good trade-off between robustness and controller complexity. Using the same method, the uncertainty weighting functions for areas 2 and 3 will be obtained.

$$\left.\begin{aligned} W_2(s) &= \frac{0.2873s + 0.0202}{s + 0.3876} \\ W_3(s) &= \frac{0.2655s + 0.0195}{s + 0.3721} \end{aligned}\right\} \quad \cdots\cdots (21)$$

The selection of constant weights η_{1i}, η_{2i} and η_{3i} is dependent on specified performance objectives and must be chosen by designer. In fact an important issue with regard to

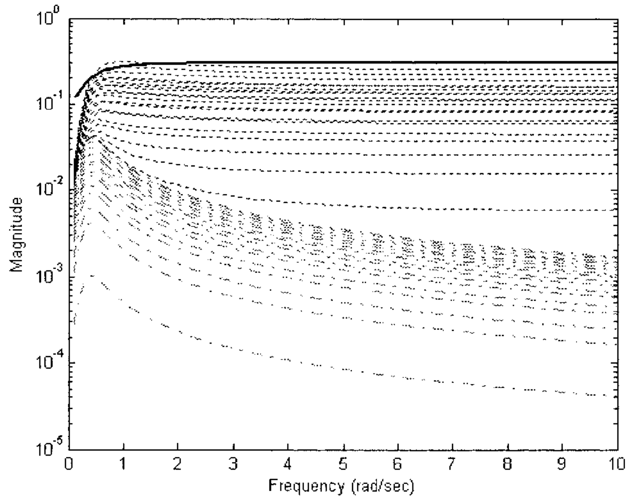

Fig. 5. Uncertainty plots; D_1 (dotted), M_1 (dash-dotted) and W_1(solid)

Table 1. Robust performance indices

Performance index	Area1	Area 2	Area 3
γ_2 (Original)	0.7439	0.7366	0.7155
γ_∞ (Original)	0.4513	0.4462	0.4326
γ_2 (Reduced)	0.7440	0.7374	0.7159
γ_∞ (Reduced)	0.4549	0.4534	0.4371

selection of these weights is the degree to which they can guarantee the satisfaction of design performance objectives. Selection of these weights entails a trade off among several performance requirements [8][14]. The coefficients η_{1i} and η_{2i} at controlled outputs set the performance goals e.t. tracking the load variation and disturbance attenuation. η_{3i} sets a limit on the allowed control signal to penalize fast change and large overshoot in the governor load set-point signal. Here, a set of suitable values for constant weights is chosen as follows:

$$\eta_{1i} = 0.25, \quad \eta_{2i} = 0.3, \quad \eta_{3i} = 0.1 \cdots\cdots\cdots\cdots (22)$$

4.2 Mixed H_2/H_∞ Control Design According to synthesis methodology described in section 3, a set of three decentralized robust controllers are designed. The problem formulation and control framework are explained in section 3. Specifically, the control design is reduced to an LMI formulation, and then the desired optimal controllers are obtained through solving the following optimization problem:

$$minimize\ \gamma_2 = \left\|T_{z_{2i}w_{2i}}\right\|_2\ subject\ to\ \gamma_\infty = \left\|T_{z_{\infty i}w_{1i}}\right\|_\infty < 1 \cdots\cdots\cdots\cdots (23)$$

The order of resulting controllers is 10 (almost it is equal to the size of area model plus $W_i(s)$). Finally, Hankel norm model reduction yielded a set of two-order controllers with virtually no performance degradation as shown in Appendix. The optimal performance indices for the original and reduced order controllers are listed in Table 1.

4.3 Pure H_∞ Control Design For the sake of comparison, in addition to proposed control strategy, a pure H_∞ dynamic output controller is developed to achieve the same objectives in each control area. With regards to specified uncertainties consider the following set of plants,

Table 2. H_∞ performance and stability indices

index	Area1	Area 2	Area 3
γ_{ST}	0.4885	0.4854	0.4585
γ_{PR}	0.9692	0.9998	0.9388

$$\Psi := \{G_i(1 + \Delta_i W_i) : \Delta_i\ \ stable, \|\Delta_i\|_\infty \leq 1\} \cdots\cdots (24)$$

Here, G_i denotes the transfer function from u_i to y_i. In order to achieve the robust performance, the H_∞ control design problem is reduced to find a controller K_i such that the closed-loop system will be internally stable for all $G_i \in \Psi$, or equivalently,

$$\gamma_{ST} = \left\|W_i K_i G_i (I + K_i G_i)^{-1}\right\|_\infty \leq 1 \cdots\cdots\cdots\cdots (25)$$

and in addition, the following performance objective will be satisfied for every $G_i \in \Psi$,

$$\gamma_{PR} = \left\|T_{z_i w_{2i}}\right\|_\infty \leq 1 \cdots\cdots\cdots\cdots\cdots\cdots (26)$$

where $T_{z_i w_{2i}}$ is the transfer function from w_{2i} to z_i, and $z_i = z_{2i}$. The resulted controllers are obtained in the following state-space form, whose order are the same as generalized area model (here 10) and the resulted robust stability and performance indices are given in Table 2.

$$\left.\begin{array}{l} \dot{x}_{ki} = A_{ki}x_{ki} + B_{ki}y_i \\ u_i = C_{ki}x_{ki} + D_{ki}y_i \end{array}\right\} \cdots\cdots\cdots\cdots\cdots\cdots (27)$$

5. Simulation Results

In order to demonstrate the effectiveness of the proposed control strategy, some simulations were carried out. In these simulations, the proposed reduced-order controllers were applied to the three control area power system described in Fig. 4. The performance of the closed-loop system using the designed reduced-order mixed H_2/H_∞ controllers in comparison of full-order pure H_∞ controllers is tested for the various scenarios of load demands, disturbances and uncertainties. Here, because of lack of space, the system responses are only shown for two sever operating conditions.

Case 1: In this case, the closed-loop performance is tested in the presence of both step load demand and uncertainties. It is assumed a large load demand 100 MW is requested by each Disco, following 20% decrease in uncertain parameters D_i and M_i. Furthermore, assume Discos contract with the available Gencos according to the following *GPM*,

$$GPM^T = \begin{bmatrix} 0.3 & 0 & 0.25 & 0 & 0.2 & 0 & 0 & 0.25 & 0 \\ 0 & 0.2 & 0 & 0 & 0.1 & 0.3 & 0 & 0.4 & 0 \\ 0 & 0.25 & 0 & 0 & 0.4 & 0 & 0 & 0 & 0.35 \end{bmatrix}$$

Gencos 4 and 7 do not participate in LFC task at all; Gencos 1, 3, 6 and 9 only participate for performing the LFC in their areas, while other Gencos track the load demand in their areas and/or others. Frequency deviation (Δf) and area control error (*ACE*) of closed-loop system are shown in Fig. 6. Using the proposed method, the area control error and frequency deviation of all areas are quickly driven back to zero. The tie-line power flows and generated powers are properly convergence to specified values as shown in Figs. 7 and 8. The actual generated powers of Gencos, according to

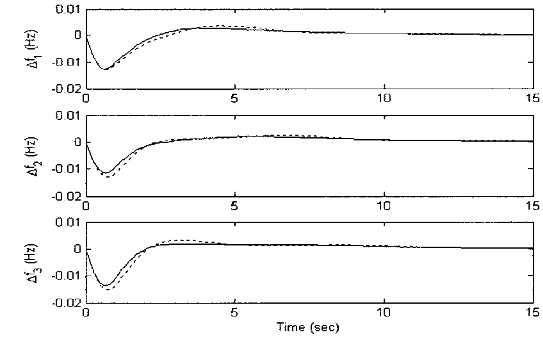

(a)

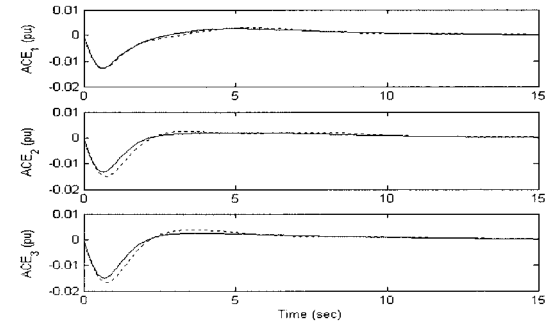

(b)

Fig. 6. System response for Case 1: (a) Frequency deviation, (b) area control error; Solid (mixed H_2/H_∞), dotted (H_∞)

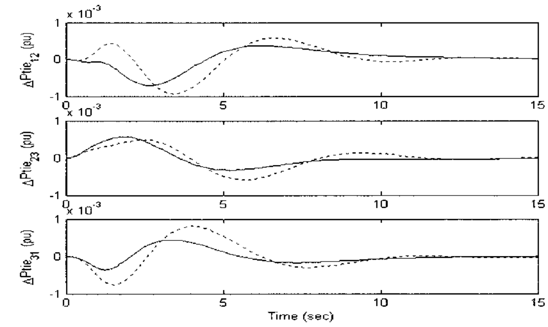

Fig. 7. Tie-line powers for Case 1; Solid (mixed H_2/H_∞), dotted (H_∞)

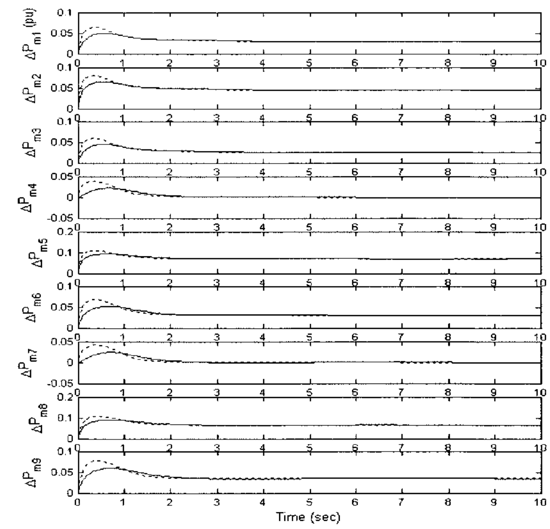

Fig. 8. Power changes for Case 1; Solid (mixed H_2/H_∞), dotted (H_∞)

Eq. (10), reach the desired values in the steady state.

Genco	1	2	3	4	5	6	7	8	9
ΔPmi *(pu)*	0.03	0.045	0.025	0	0.07	0.03	0	0.065	0.035

Fig. 8 shows the power is initially coming from all Gencos to respond to the load increase which will result in a frequency drop that is sensed by the governors of all machines. But at steady state the necessary powers are coming from Gencos which participate in LFC task. Since the total exported and imported powers for each control area are equivalent, the scheduled steady state power flows over the tie lines are zero. Comparing the simulation results with both types of controllers, shows that the proposed design achieves better frequency regulation with small settling times.

Case 2: Consider the case 1 again. Assume in addition to

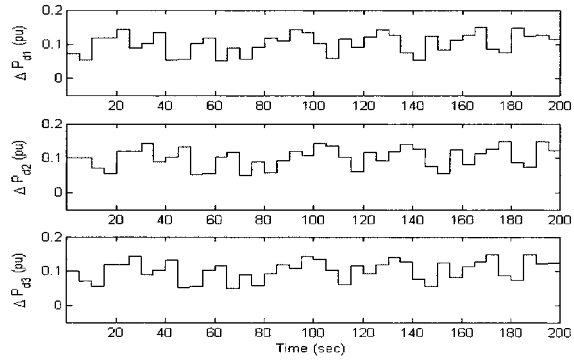

(a)

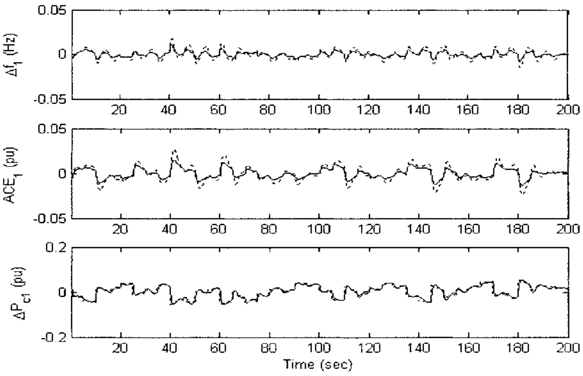

(b)

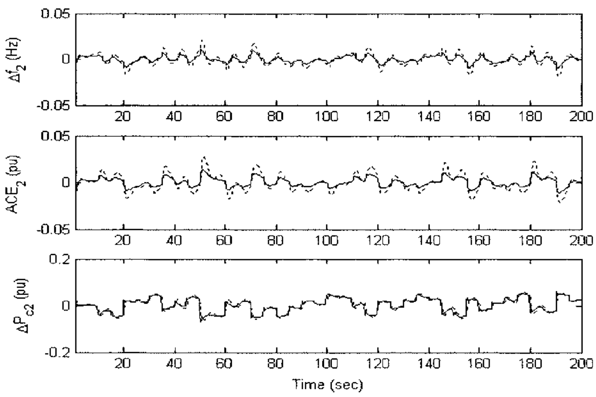

(c)

Fig. 9. System response for Case 2: (a) Random load patterns, (b) Area-1, (c) Area-2; Solid (mixed H_2/H_∞), dotted (H_∞)

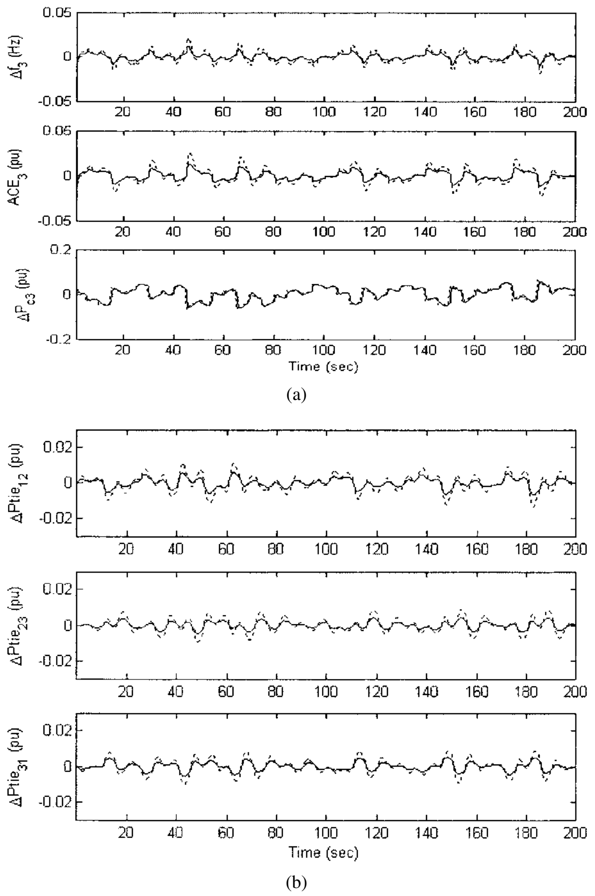

Fig. 10. System response for Case 2: (a) Area-3, (b) Tie-line powers; Solid (mixed H_2/H_∞), dotted (H_∞)

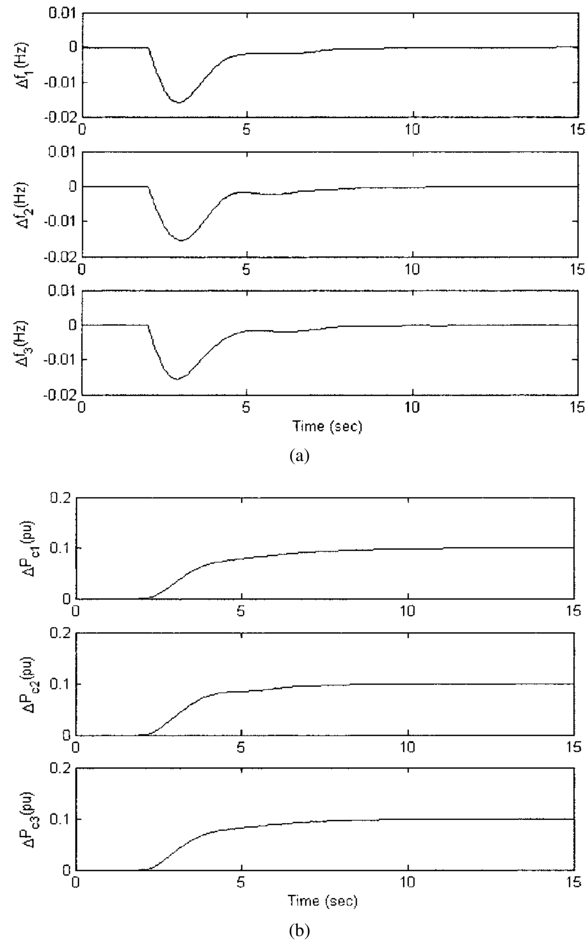

Fig. 11. System response for Case 1; (η_{3i}=0.5): (a) Frequency deviation, (b) Control effort signal

specified contracted load demands and 20% decrease in uncertain parameters, a bounded random step load change as a large uncontracted demand (shown in Fig. 9(a)) is appears in each control area, where

$$-50\,\text{MW}(-0.05\,\text{pu}) \le \Delta P_{di} \le +50\,\text{MW}(+0.05\,\text{pu})$$

The purpose of this scenario is to test the robustness of the proposed controllers against uncertainties and random large load disturbances. The control area responses are shown in Figs. 9, 10.

These figures demonstrate that the designed controllers track the load fluctuations and meet robustness, effectively. Simulation results show the validity of generalized LFC model and demonstrate the proposed low-order mixed H_2/H_∞ controllers perform the closed-loop performance better than the full-order H_∞ controllers for a wide range of load disturbances, uncertainties and possible bilateral contract scenarios. It can be seen that proposed design gives small frequency deviation amplitude using less control effort with smooth changes, which is more useful in real-world LFC applications.

It is notable that with the existing limits on the rate and range of generation change and the fact that steam units (for example) take a few to several dozen seconds to fully respond, maneuvering generation to mach fast varying components of area demand is impossible [16]. In light of this direction, the proposed control strategy includes enough flexibility to set a desired level of performance to cover the practical constraint on control action signal. It is easily carried out by tuning of η_{3i} in the fictitious controlled output $z_{2i}(3)$ shown in Fig. 2. Specifically, by increasing the weight of η_{3i}, we can obtain a more smooth control signal. For instance, by changing η_{3i} from 0.1 to 0.5, the system response (frequency deviation and control signals) for Case 1 will be obtained as shown in Fig. 11 (to see the response clearly, the start up time is moved to 2 second).

Fig. 11 shows that although the applied step load disturbance includes fast changes in its amplitude at 2 second (from 0.0 to 0.1 pu), however the proposed controllers penalize the fast change and overshoot in the governor set-point signals ΔP_{ci}, effectively.

6. Conclusion

Since in real-world restructured power system, each control area is faced with various uncertainties and disturbances, the LFC problem in a multi-area power system is formulated as a decentralized multi-objective optimization control problem. A mixed H_2/H_∞ technique is used to design the desired controllers. The proposed method was applied to a three control area power system and is tested under various possible scenarios. The results are compared with the results of applied dynamic output H_∞ controllers. Simulation results demonstrated the effectiveness of proposed methodology.

Acknowledgment

The authors would like to thank the reviewers for their constructive comments and suggestions.

(Manuscript received Feb. 9, 2004,
revised June 2, 2004)

References

(1) J. Kumar, NG.K. Hoe, and G.B. Sheble: "AGC simulator for price-based operation, Part 1: A model", *IEEE Trans. Power Syst.*, Vol.2, No.12, pp.527–532 (1997)

(2) J. Kumar, NG.K. Hoe, and G.B. Sheble: "AGC simulator for price-based operation, case study results", *IEEE Trans. Power Syst.*, Vol.2, No.12, pp.533–538 (1997)

(3) V. Donde, M.A. Pai, and I.A. Hiskens: "Simulation and optimization in a AGC system after deregulation", *IEEE Trans. Power Syst.*, Vol.16, No.3, pp.481–489 (2001)

(4) B. Delfino, F. Fornari, and S. Massucco: "Load-frequency control and inadvertent interchange evaluation in restructured power systems", *IEE Proc.-Gener. Transm. Distrib.*, Vol.149, No.5, pp.607–614 (2002)

(5) H. Bevrani, Y. Mitani, and K. Tsuji: "Robust AGC: Traditional structure versus restructured scheme", *IEEJ Trans. PE*, Vol.124-B, No.5, pp.751–761 (2004)

(6) H. Bevrani, Y. Mitani, and K. Tsuji: "Robust decentralized AGC in a restructured power system", *Energy Conversion* & *Management*, Vol.45, No.15-16, pp.2297–2312 (2004)

(7) A. Feliachi: "Reduced H∞ Load Frequency Controller in a Deregulated Electric Power System Environment", Proc. of the Conference on Decision & Control, pp.3100–3101, California, USA (1997)

(8) H. Bevrani, Y. Mitani, and K. Tsuji: "On robust load-frequency regulation in a restructured power system", *IEEJ Trans. PE*, Vol.124-B, No.2, pp.190–198 (2004-2)

(9) D. Rerkpreedapong, A. Hasanovic, and A. Feliachi: "Robust load frequency control using genetic algorithms and linear matrix inequalities", *IEEE Trans. Power Syst.*, Vol.18, No.2, pp.855–861 (2003)

(10) K. Zhou, K. Glover, B. Bodenheimer, and J. Doyle: "Mixed H_2 and H_∞ performance objectives I: Robust performance analysis", *IEEE Trans. Automat. Control*, Vol.39, No.8, pp.1564–1574 (1994)

(11) M. Chilali and P. Gahinet: "H_∞-design with pole placement constraints: An LMI approach", *IEEE Trans. Automat Control*, Vol.41, No.3, pp.358–367 (1996)

(12) P.P. Khargonekar and M.A. Rotea: "Mixed H_2/H_∞ control: A convex optimization approach", *IEEE Trans. Automat Control*, Vol.36, No.7, pp.824–837 (1991)

(13) C. Scherer: "Multiobjective H_2/H_∞ control", *IEEE Trans. Automat Control*, Vol.40, pp.1054–1062 (1995)

(14) H. Bevrani, Y. Mitani, and K. Tsuji: "Sequential design of decentralized load-frequency controllers using μ-synthesis and analysis", *Energy Conversion* & *Management*, Vol.45, No.6, pp.865–881 (2004)

(15) T. Kennedy, S.M. Hoyt, and C.F. Abell: "Variable nonlinear tie-line frequency bias for interconnected system control", *IEEE Trans. Automat. Control*, Vol.3, pp.1244–1253 (1988)

(16) N. Jaleeli, D.N. Ewart, and L.H. Fink: "Understanding automatic generation control", *IEEE Trans. Power Syst.*, Vol.7, No.3, pp.1106–1112 (1992)

Appendix

State-space model of load-frequency controllers:

$$\dot{x}_{ki} = A_{ki}x_{ki} + B_{ki}y_i$$

$$u_i = C_{ki}x_{ki} + D_{ki}y_i$$

Where,

$$A_{k1} = \begin{bmatrix} -4.3157 & 1.2354 \\ 1.2269 & -0.9023 \end{bmatrix}, B_{k1} = \begin{bmatrix} 4.9573 & 1.7128 \\ -0.8207 & -0.1915 \end{bmatrix}$$

$$C_{k1} = \begin{bmatrix} 5.2449 & -0.8427 \end{bmatrix}, D_{k1} = \begin{bmatrix} -7.3060 & -2.9997 \end{bmatrix}$$

$$A_{k2} = \begin{bmatrix} -4.0991 & 1.4551 \\ 1.4357 & -1.0581 \end{bmatrix}, B_{k2} = \begin{bmatrix} -4.4945 & -1.6576 \\ 0.9659 & 0.2106 \end{bmatrix}$$

$$C_{k2} = \begin{bmatrix} -4.7904 & 0.9886 \end{bmatrix}, D_{k2} = \begin{bmatrix} -6.7670 & -2.9912 \end{bmatrix}$$

$$A_{k3} = \begin{bmatrix} -4.0994 & 1.5063 \\ 1.4880 & -1.0972 \end{bmatrix}, B_{k3} = \begin{bmatrix} 4.4458 & 1.6168 \\ -0.9935 & -0.2199 \end{bmatrix}$$

$$C_{k3} = \begin{bmatrix} 4.7306 & -1.0175 \end{bmatrix}, D_{k3} = \begin{bmatrix} -6.6820 & -2.9927 \end{bmatrix}$$

Hassan Bevrani (Student Member) received his M.Sc degree (first class honors) in Electrical Engineering from K. N. Toosi University of Technology, Tehran, Iran in 1997. He is currently a Ph.D student at Osaka University. His special fields of interest included robust control and modern control applications in Power system and Power electronic industry. He is a student member of the Institute of Electrical Engineers of Japan, IEE, and IEEE.

Yasunori Mitani (Member) received his B.Sc., M.Sc., and Dr. of Engineering degrees in electrical engineering from Osaka University, Japan in 1981, 1983, and 1986 respectively. He joined the Department of Electrical Engineering of the same university in 1990. He is currently a professor in Kyushu Institute of Technology. His research interests are in the areas of analysis and control of power systems. He is a member of the Institute of Electrical Engineers of Japan, the Institute of Systems, Control and Information Engineers of Japan, and the IEEE.

Kiichiro Tsuji (Member) received his B.Sc and M.Sc. degrees in electrical engineering from Osaka University, Japan, in 1966 and 1968, respectively, and his Ph.D in systems engineering from Case Western Reserve University, Cleveland, Ohio in 1973. In 1973 he jointed the Department of Electrical Engineering, Osaka University, and is currently a professor at Osaka University. His research interests are in the areas of analysis, planning, and evaluation of energy systems, including electrical power systems. He is a member of the Institute of Electrical Engineers of Japan, the Japan Society of Energy and Resources, the Society of Instrument and Control Engineers, the Institute of Systems, Control and Information Engineers, and the IEEE.